SolarPACES 2022, 28th International Conference on Concentrating Solar Power and Chemical Energy Systems
Operations, Maintenance, and Component Reliability
https://doi.org/10.52825/solarpaces.v1i.711

Published: 04 Mar. 2024

Investigating Various Failure Models on Commercial Silicon Carbide

Pawan Chaugule[1][https://orcid.org/0000-0002-7570-6572], Mark C. Messner[1][https://orcid.org/0000-0002-0040-4385], Bipul Barua[1][https://orcid.org/0000-0002-4718-4113], and Dileep Singh[1]

[1] Argonne National Laboratory, United States of America

Abstract. Structures and components made from ceramic materials are often brittle and can fail by the unstable growth of existing flaws such as voids and cracks. There have been several failure criteria developed for ceramics, in the past and they are broadly categorized based on their dependency on crack geometry. The present work implements eight failure criteria using an open-source software package – *srlife,* which predicts the lifetime or failure probability of concentrated solar power (CSP) structural components. The present work also checks the viability of building a ceramic CSP receiver, by analyzing the reliability predictions from *srlife* for a SiC ceramic. The reliability predictions for a biaxial loading problem indicated the Shetty Mixed-Mode criterion gives the most conservative predictions. Whereas, in case of the CSP receiver, the predictions show that the co-planar strain energy criterion gives the most conservative predictions as it is agnostic towards the type of stress, and therefore, is not recommended to be used designing ceramic receivers.

Keywords: Probability Predictions, Reliability, Concentrated Solar Power, Ceramics

1. Introduction

Current concentrated solar power (CSP) systems as well as next generation, higher temperature CSP concept designs, use or target metallic receivers [1]. However, for next generation, high temperature designs, the estimated design life of metal components is shown to decrease with increasing operating temperature and stress levels, as a result of reduction in creep and rupture strength [2]. Advanced ceramics could be a better alternative to metal alloys, such as Nickel based superalloys, in designing the CSP components. Ceramics are known to possess excellent high temperature strength, relatively low thermal expansion and, hence, can function at relatively higher temperatures for longer periods of time [3]. However, ceramic materials offer manufacturing challenges such as limited ductility and difficulties in fabricating and joining ceramic components to other power plant components. Additionally, engineers need the ability to predict the reliability of ceramics operating in CSP environments to assess the economics of the system.

Structures and components made from ceramic materials are often brittle and can fail by the unstable growth of existing flaws such as voids and cracks. The failure of ceramic materials is stochastic in nature because of the variable severity of the pre-existing flaws. The failure data from several (repeated) experiments can be fitted with statistical distributions such as the Weibull distribution [4]. The distribution aids in fast-fracture reliability analysis of ceramics subjected with uniaxial stresses. In case of polyaxial stresses, different failure criteria and flaw geometries can be incorporated into the distribution expression, to extend the uniaxial failure model to arbitrary states of stress while accounting for the size effect, thus, improving the reliability/failure probability prediction.

In the past, several failure criteria and concepts have been formulated depending on loading conditions and dominating modes of failure which led to crack growth in a time-independent and time-dependent manner. Some of these criteria/concepts include: (i) Principal of Independent Action (PIA) method, (ii) Weibull normal tensile stress averaging (WNTSA) method, (iii) Maximum tensile stress (MTS) criterion, (iv) Total coplanar strain energy (CSE) release rate criterion, and (iv) Shetty's Mixed Mode (SMM) criterion. In the present work we implement these criteria to predict time-independent failure. Future extensions of the work will consider time-dependent failure. A demonstration of all these criteria has been shown by NASA in the Ceramics Analysis and Reliability Evaluation of Structures Life Prediction Program (CARES)[5], [6], [7]. The demonstration includes an example problem which is used in verifying the models implemented in the present work.

The present work reanalyses the example problem by implementing the failure criteria as extension models to *srlife* – an open-source software package for evaluating the life of high temperature CSP components [8]. On verifying the results of the extension models, the viability of a SiC CSP receiver is investigated by evaluating its reliability using the various models in *srlife*. Based on the reliabilities, recommendations are made on the models appropriate for reliability analyses of ceramic receivers, based on available failure data.

2. Ceramic Failure Models

The models mentioned in the introduction begin by using uniaxial failure statistics for a heat of ceramic material, for instance flexure strengths quantified from a series of three-point or four-point bend tests [9], [10]. The models aim to predict fast-fracture under arbitrary stress states and account for the size effect in ceramics. The size effect describes how it is more likely to find a critical flaw as the sample volume becomes larger. That is, for ceramics, larger equals weaker. Figure 1 shows a taxonomy of the models considered in the present study.

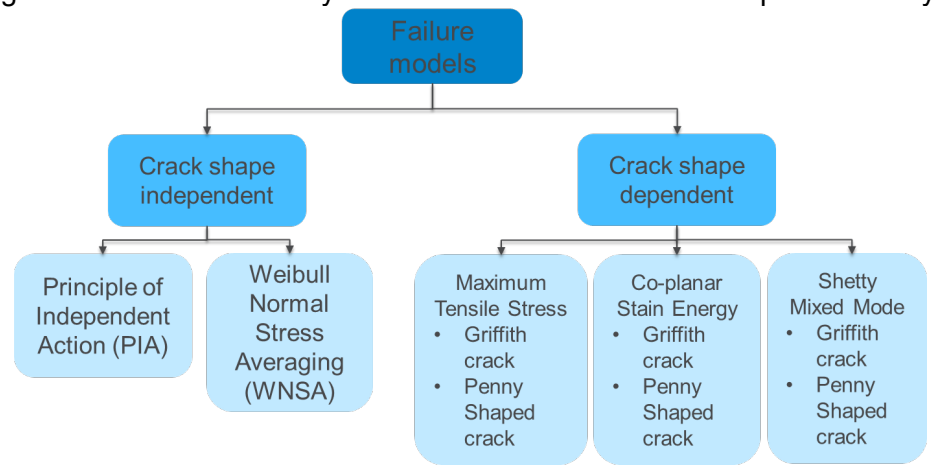

Figure 1. Flow chart of failure models considered in present study.

The flow chart differentiates the models based of their dependency on the crack shape (Griffith cracks and penny shaped cracks) and fracture criteria which account for polyaxial stresses. The polyaxial stresses are provided by the structural analyses in *srlife*. A two-parameter Weibull model coupled with the above fracture criteria is used in the reliability predictions, with the assumption that all the failure causing flaws are volume based as shown in Eq. 1. The statistical material parameters are estimated directly from flexural or uniaxial tests which are Weibull modulus (m_v) and characteristic strength ($\sigma_{\theta v}$). Using them the scale parameter (σ_{0v}), and uniaxial Batdrof crack density coefficient (k_{wv}) are derived in Eq. 2 where V = b*d*l_0 is the gauge volume. Table 1 and 2 list the constitutive equations of the failure models implemented.

$$P_{fV} = \begin{cases} 1 - exp\left(- \int_V \left(\frac{\sigma}{\sigma_{0v}} \right)^{m_V} \mathrm{d}V \right) & if \quad \sigma > 0 \\ 0 \quad if \quad \sigma \leq 0 \end{cases} \tag{1}$$

$$\sigma_{0v} = \sigma_\theta \left(\frac{V*\left(\left(\frac{l}{L}\right)*m_v+1\right)}{2*(m_v+1)^2} \right)^{\frac{1}{m_v}} \quad \text{and} \quad k_{wv} = (\sigma_{0v})^{-m_v} \qquad \text{(2) and (3)}$$

Table 1. Constitutive equations for the crack shape independent models.

Crack shape independent models	Probability of failure	Eq.
1. Principle of Independent Action (PIA)	$P_{f_V} = 1 - exp\left(-k_{w_V} \sum_i^n (\sigma_1^{m_V} + \sigma_3^{m_V} + \sigma_3^{m_V}) \Delta V_i \right)$	(4)
2. Weibull Normal Stress Averaging (WNSA)	$\boldsymbol{P_{f_V} = 1 - exp\left(-k_{wpv} \sum_i^n (\overline{\sigma_n}^{m_V}) \Delta V_i \right)}$	(5)
	$\boldsymbol{k_{wpv} = (2m_v + 1)\, k_{w_V}}$	(6)
	Avereage normal tensile stress $\boldsymbol{\overline{\sigma_n}^{m_V} = \frac{\int_A \sigma_n{}^{m_V}\, dA}{\int_A dA}}$	(7)

Table 2. Constitutive equations for the crack shape dependent models.

Crack shape dependent models			Eq.
Probability of failure		$P_{f_V} = 1 - exp\left\{ -\frac{2k_{Bv}}{\pi} \sum_{i=1}^n V_i \left[\int_A \sigma_e^{m_v}(\alpha,\beta) dA \right]_i \right\}$	(8)
Normal stress		$\sigma_n = \sigma_1 l^2 + \sigma_2 m^2 + \sigma_3 n^2$	(9)
Shear stress		$\tau^2 = \sigma^2 - \sigma_n^2$	(10)
Fracture criteria	Crack geometry	Effective stress	
3. Maximum tensile stress criterion [6]	Griffith flaw (GF)	$\sigma_e = \frac{1}{2}\left\{ \sigma_n + \sqrt{\sigma_n^2 + \tau^2} \right\}$	(11)
	Penny shaped flaw (PSF)	$\sigma_e = \frac{1}{2}\left\{ \sigma_n + \sqrt{\sigma_n^2 + \left(\frac{\tau}{1-0.5v}\right)^2} \right\}$	(12)
4. Total co-planar strain energy release rate criterion [6]	Griffith flaw	$\sigma_e = \sqrt{\sigma_n^2 + \tau^2}$	(13)
	Penny shaped flaw	$\sigma_e = \sqrt{\sigma_n^2 + \left(\frac{\tau}{1-0.5v}\right)^2}$	(14)
5. Shetty's mixed-mode criterion [15]	Griffith flaw	$\sigma_e = \frac{1}{2}\left[\sigma_n + \sqrt{\sigma_n^2 + \left(\frac{2\tau}{\bar{C}}\right)^2} \right]$	(15)
	Penny shaped flaw	$\sigma_e = \frac{1}{2}\left[\sigma_n + \sqrt{\sigma_n^2 + \left(\frac{4\tau}{\bar{C}(2-\nu)}\right)^2} \right]$	(16)

The terms used in the equations are; k_{wpv}: polyaxial Batdorf coefficient, k_{Bv}: material Batdorf coefficient, V_i: element volume, (α, β) : orientations of elemental surface area dA, $(\mathrm{l}, \mathrm{m}, \mathrm{n})$:

direction cosines of traction vector σ, υ: Poisson ratio, and $\bar{C}$:in Shetty's model is the empirical constant adjusted to best fit the data. Shetty found a range values of $0.8 \leq \bar{C} \leq 2.0$ for materials such as soda-lime glass and various ceramics with large cracks. *Note*: In the PIA model, the terms σ_i are the tensile principal stresses. The compressive principal stresses are taken to be zero as they are not assumed to contribute to the failure probability. Whereas, in the rest of the models, as per the CARES manual specification, when a principal compressive stress exceeds the maximum principal tensile stress (for the same element) by a factor of three, the corresponding reliability is set to unity.

3. Model Verification

The verification of the above models implemented in *srlife* is done by simulating an example problem presented in CARES manual and comparing the failure predictions between the models in CARES and *srlife*, respectively. The problem statement is as follows. A circular disk made of Alumina is transversely loaded as demonstrated experimentally in Rufin and Bollard [7]. The material properties are: Youngs modulus = 405 GPa, Poisson ratio = 0.25. The Weibull parameter for Alumina from separate flexure strength test data [6] are estimated as: m_V = 28.53, σ_0 = 169.7 $MPa\ m^{3/28.53}$ or 350.8 $MPa\ mm^{3/28.53}$,$k_{wpv} = 58.06$. The disk was loaded in the experiment from 1.24 MPa to 1.79MPa. To simulate the disk loading a finite element (FE) method was implemented in the CARES manual, on a 7.5 degree segment of the disk, and the failure probability was evaluated from the stresses obtained. For the *srlife* model verification a FE method was implemented on a disk segment of 45 degrees as shown in Fig. 2 and the failure probability was obtained similarly.

In Fig. 3, a comparison plot between the results obtained from CARES and using *srlife* are shown. As observed from the data and plots, the results from *srlife* match with those from CARES manual. On the basis of this comparison, it is conclude that all the ceramic failure models shown in the flowchart are correctly implemented. The plot in Fig. 3 also shows that the order of failure probability followed by the models is as follows:

PIA < WNTSA < MTS_GF < MTS_PSF < CSE_GF < CSE_PSF < SMM_GF < SMM_PSF

and the Shetty model for the PSF is observed to be the most conservative.

4. Reliability Model Comparison for Ceramic Receivers

In this section, we assess the failure models in terms of their applicability and conservativeness for designing high temperature ceramic receivers. We created a reference receiver model for this assessment. The reference model is an 8.5 m diameter, 10.5 m tall, 360° external cylindrical receiver with a thermal design power of 120 MW_t and maximum flux limit of 1.0 kW/m^2. We considered 32% $MgCl_2$ / 68% KCl eutectic molten salt as the heat transfer fluid (HTF). We used DELSOL3 [11] to determine the incident heat flux on the receiver. Figure 4 shows the heat flux map on the receiver at noon and the variation in heat flux during the day. The figure also plots the variation in HTF mass flow rate, determined iteratively to achieve nearly constant outlet temperature of 720 °C throughout the day. The HTF enters the receiver at 550 °C from the north side, flows through two serpentine flow paths, each containing 9 panels, and leaves the receiver at the south side. Each panel contains 32 tubes with 1 mm thickness and 42.2 mm outer diameter. We considered a design fluid pressure of 2 MPa. The tube material is SiC.

Given the flux input data, tube geometry, mass flow rate, and pressure load, *srlife* performs thermohydraulic analysis to determine tube temperature history, performs structural analysis using temperature and pressure to determine stress history, and finally computes reliability of individual tubes using stress and temperature histories. Details of the thermohydraulic analysis and reliability analysis modules, recently added in *srlife*, can be found

in a companion paper [12]. The structural analysis module along with the overall structure of *srlife* are discussed in [8]. Thermo-physical properties of the HTF and thermal and structural properties of SiC were collected from literature and can be found in the material database of *srlife*, available at https://github.com/Argonne-National-Laboratory/srlife. We modeled the deformation of SiC as linear-elastic.

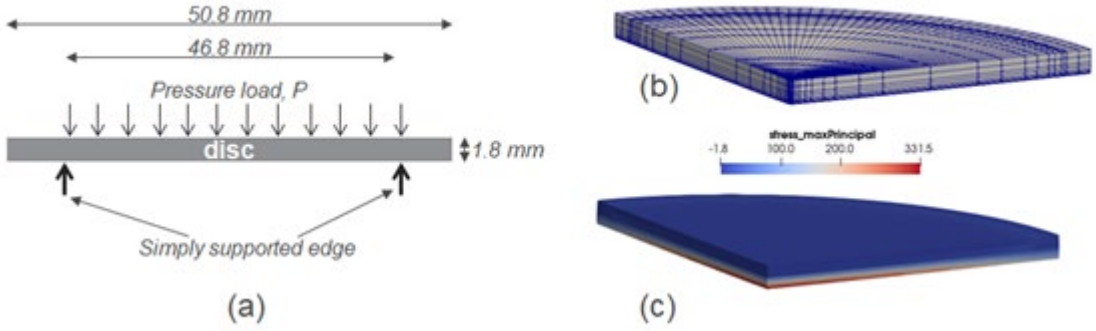

Figure 2. (a) Geometry, loading, and boundary condition (b) quarter symmetry 3D finite element model, and (c) example results from structural analysis of the transversely loaded circular disc example provided in CARES/LIFE manual [5,6].

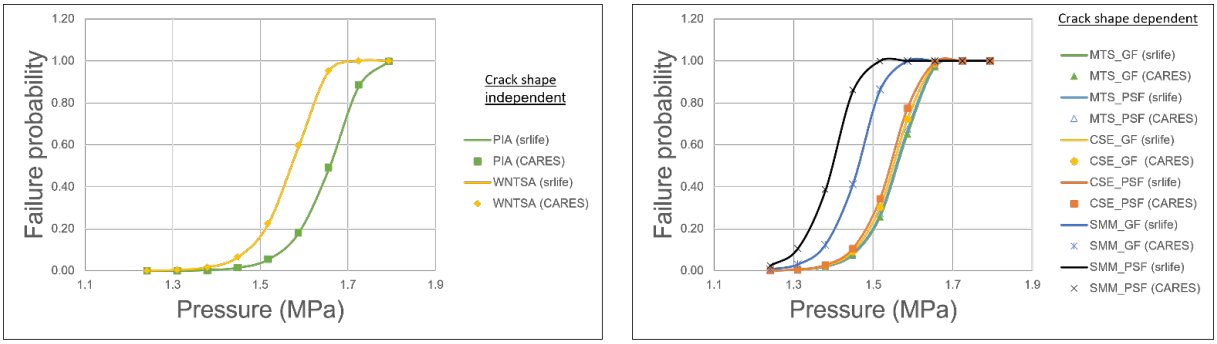

(a) (b)

Figure 3. Comparison of failure probabilities from CARES manual (symbols) and *srlife*, generated using the models (a) PIA, WNTSA (b) MTS, CSE, and SMM for penny-shaped flaw (PSF) and griffith flaw (GF).

Analysing all the tubes in a receiver is expensive. Previous work [13] on metallic receivers indicates conservative estimation of life when structural analysis is performed considering only the hottest and coldest tubes in a panel. For structural analysis, we also considered all the panels are mechanically decoupled but tubes in a panel are rigidly connected to the tube manifold. Figure 5 shows the temperature and axial stress distribution in the hottest tube of individual panels in the receiver at noon. The maximum tube temperature in the receiver is about 800 °C. The axial stress component in the tubes is significantly higher than the other stress components (not shown in the figure) which is expected, especially for external receivers. In addition to the axial constant by the tube manifold, tubes in an external receiver are subjected to the circumferentially large temperature difference. The structural analysis results also indicate that the high stress locations in the tubes are mostly compressive. This has an important significance on selecting the appropriate failure model for designing ceramic receivers, as ceramic materials are much stronger in compression than tension.

Using the stress results *srlife* performs the reliability analysis of individual tubes using the ceramic failure model selected by the user. Time-independent reliability analysis requires Weibull parameters m and σ_0 of the material for all the models discussed above. The values

of m and σ_0 for SiC are from [14] and listed in Table 3. The SMM model requires an additional parameter $\bar{C}$, which can be determined from fracture tests in mixed mode condition. The value of $\bar{C}$ is not available for SiC. To be able to use SMM model, however, we considered $\bar{C} = 1.5$, a value in the range of $0.8 \leq \bar{C} \leq 2.0$ found by Shetty [15] for ceramic materials.

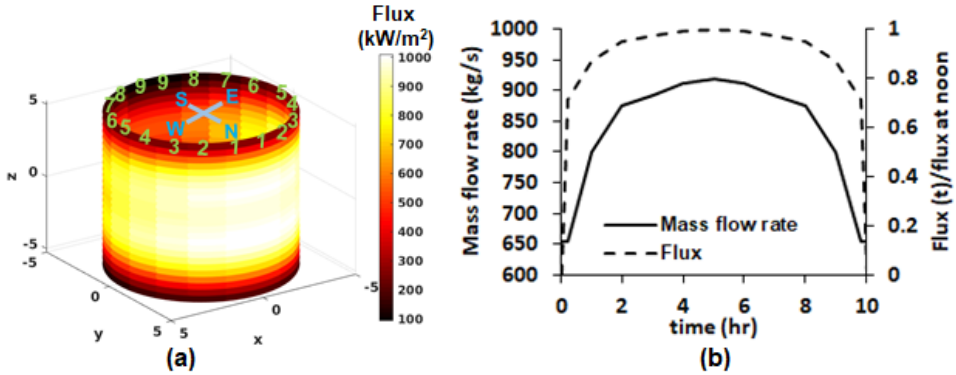

Figure 4. (a) Heat flux map on the receiver at noon. Numbers 1 to 9 indicates panels along two flow paths. (b) Variation in heat flux and heat transfer fluid mass flow rate during the day.

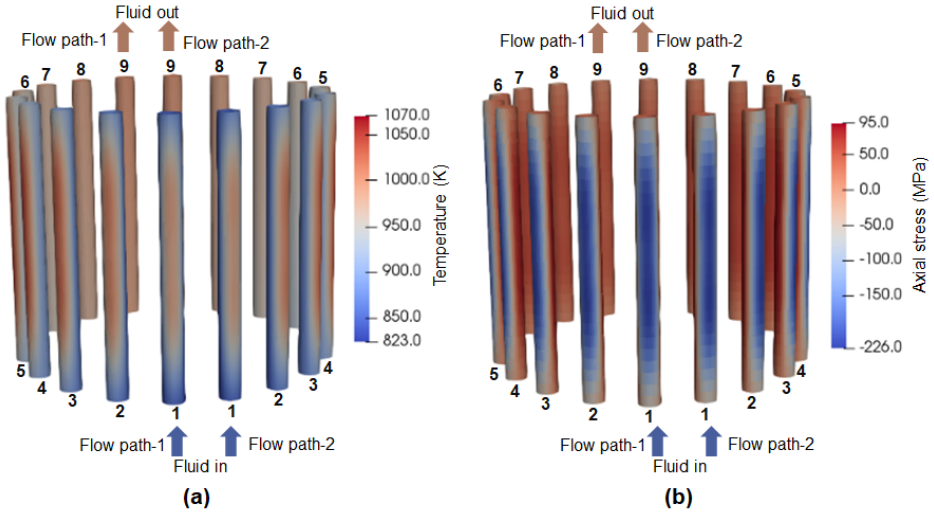

Figure 5. (a) Temperature and (b) axial stress distribution in one of the two tubes per panel considered in thermohydraulic and structural analyses.

Temperature (°C)	Weibull modulus, m	Scale parameter, σ_0 (MPa-(mm)^(3/m))
25	10.70	507
800	10.70	467

Table 3. Weibull parameters of SiC [14].

Figure 6 compares the minimum tube reliabilities among different failure models. The minimum tube reliability is based on the minimum value of reliability among all the tubes in the receiver during the load cycle. The figure ranks the model in terms of their conservatism in calculating reliability of receiver tubes:

PIA < WNTSA < MTS_GF < MTS_PSF < SMM_GF < SMM_PSF< CSE_GF < CSE_PSF

This order is different than the order found for the transversely loaded circular disc example problem (Fig. 3). The SMM models calculate the least reliability for the circular disc problem, while the CSE models calculate the least reliability for the receiver tubes. This discrepancy, we believe, is due to an inherent flaw in the CSE models. The effective stress formulations in the CSE models (Eq. 12 and Eq. 13) are agnostic towards the type of stress, as they are

always calculated based on positive values of the normal and shear stresses, even if the stresses are compressive in nature.

As Figure 5b indicates, the receiver tubes experience compressive stresses at many locations and therefore CSE models calculate much lower reliability than other models. We therefore do not recommend CSE models for reliability analysis of ceramic receivers. All of the remaining models are reasonable for use in design evaluations. The SMM models are most conservative but require $\bar{C}$ to be determined from biaxial failure data. We recommend the use of this model if $\bar{C}$ is available for the tube material. If it is not available, we recommend the MTS model based on its simplicity as it does not require multiaxial failure data.

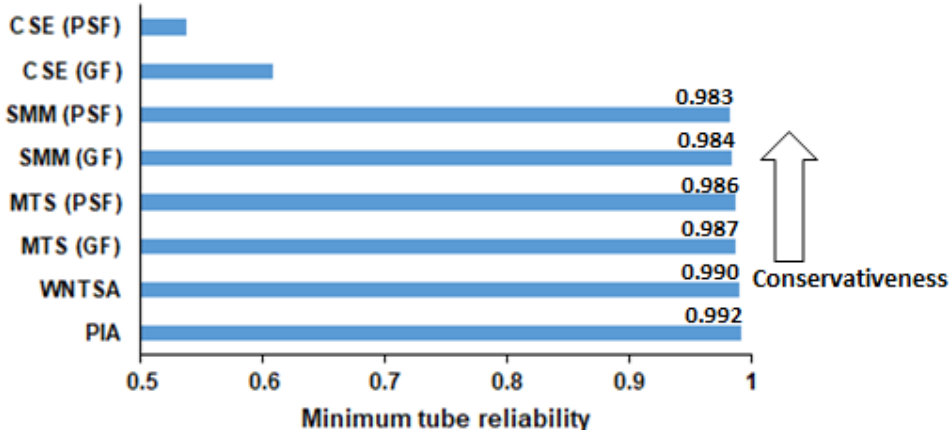

Figure 6. Minimum tube reliability vs ceramic failure model.

5. Conclusions

The present work demonstrates the time-independent reliability analysis of a ceramic CSP receiver using the *srlife* tool. The reliability analysis was conducted using eight different failure models added as extensions to *srlife*. The models were compared based on their reliability predictions and recommendations were made. The Shetty Mixed-Mode model generates the most conservative predictions (from the biaxial loading problem) and, hence, can be used if the parameter $\bar{C}$ is known. If the parameter is unknown the maximum tensile stress model can be used. The co-planar strain energy model is not recommended to be used in cases when large compressive stresses are present, as it is agnostic towards the type of stress.

Data availability statement

The material data used in the sample receiver problem is contained in the distribution of the srlife software, available at https://github.com/Argonne-National-Laboratory/srlife.

Underlying and related material

The source code for srlife and the input data for various examples are available at https://github.com/Argonne-National-Laboratory/srlife.

Author contributions

P. C. added the ceramic failure models to srlife and contributed to the initial and final drafts of the manuscript. M. C. M. modified the srlife software. B. B. ran the example analysis and helped write the draft and final manuscripts. D. S. helped administer the project and collect ceramic failure data. All reviewed and edited the final manuscript.

Competing interests

The authors declare no competing interests.

Funding

This work was sponsored by the U.S. Department of Energy, under Contract No. DE-AC02-06CH11357 with Argonne National Laboratory, managed and operated by UChicago Argonne LLC. Funding was provided by the U.S. Department of Energy, Office of Energy Efficiency and Renewable Energy, Solar Energy Technologies Office, Concentrating Solar Power Program, under award #38482.

References

1. M. Mehos *et al.*, “Concentrating Solar Power Gen3 Demonstration Roadmap,” *Nrel/Tp-5500-67464*, no. January, pp. 1–140, 2017, doi: 10.2172/1338899.
2. M. C. Messner, B. Barua, and D. Singh, “Towards a design framework for non-metallic concentrating solar power components,” *AIP Conf. Proc.*, vol. 2445, no. May, 2022, doi: 10.1063/5.0085670.
3. B. Barua, M. C. Messner, and D. Singh, “Assessment of Ti3SiC2MAX phase as a structural material for high temperature receivers,” *AIP Conf. Proc.*, vol. 2445, no. May, 2022, doi: 10.1063/5.0085952.
4. ASTM C1239, “Standard Practice for Reporting Uniaxial Strength Data and Estimating Weibull Distribution Parameters for Advanced Ceramics,” *Astm*, vol. i, no. January, pp. 1–17, 2000, doi: 10.1520/C1239-13R18.Scope.
5. N. N. Nemeth, J. M. Manderscheid, and J. P. Gyekenyesi, “Ceramics Analysis and Reliability Evaluation (CARES) Users and Programmers Manual,” 1990. doi: 10.1016/b978-1-4831-0607-6.50026-0.
6. N. N. Nemeth, L. M. Powers, L. a. Janosik, and J. P. Gyekenyesi, *CARES/LIFE Ceramics Analysis and Reliability Evaluation of Structures Life Prediction Program*, no. Feb. 2003.
7. A. C. Rufin, D. R. Samos, and R. J. H. Bollard, “Statistical failure prediction models for brittle materials,” *AIAA J.*, vol. 22, no. 1, pp. 135–140, 1984, doi: 10.2514/3.48426.
8. M. C. Messner, B. Barua, and M. D. McMurtrey, “srlife : A Fast Tool for High Temperature Receiver Design and Analysis,” 2022.
9. ASTM International, “ASTM Standard Test Method for Flexural Strength of Advanced Ceramics at Elevated Tempeartures C1211 - 18,” 2003. doi: 10.1520/C1211-18.2.
10. ASTM International, “ASTM Standard Test Method for Flexural Strength of Advanced Ceramics at Ambient Temperature C1161 - 18,” 2003. doi: 10.1520/C1161-18.1.
11. Kistler, B. L. (1986). "A user’s manual for DELSOL3: a computer code for calculating the optical performance and optimal system design for solar thermal central receiver plants". Sandia National Laboratories, Sandia Report No. SAND86-8018
12. Messner, M.C. et al. “A Computer Design Tool for Ceramic Receivers.” Submitted to the 2022 SolarPACES Conference.
13. B. Barua, M. C. Messner, “Fast Heuristics for Receiver Life Estimation and Design,” SolarPaces Conference 2021 (accepted).
14. Tanaka, T., Nakayama, H., Sakaida, A., & Imamichi, T. (1995). "Evaluation of Weibull parameters for static strengths of ceramics by Monte Carlo simulation." Journal of the Society of Materials Science, Japan, 44(498Appendix), 51-58.
15. D. K. Shetty, “Mixed-Mode Fracture Criteria for Reliability Analysis and Design With Structural Ceramics,” vol. 109, (1987).